Magnetorotational instability: a review

David Larson, Wonjae Lee, and Shi Sim
University of California, San Diego

(Received 9 June 2013)

We review magnetorotational instability and its role in transporting angular momentum within accretion disks. Theoretical, experimental and numerical simulation research work is surveyed.

CONTENTS

1. Introduction

Turbulence generating magnetorotational instability (MRI) was first discovered by Velikhov (1959) and Chandrasekhar (1960), and was later re-discovered by Balbus & Hawley (1998) for astrophysical applications. MRI has since then been confirmed by robust numerical simulations, but to date has not been verified experimentally or through observations. To understand the importance of MRI, we have to look into the accretion disk theory where many astrophysical phenomena take place in.

Accretion disks are disk made up of gas, dust, and plasma that rotates around and gradually collapses onto an object in the center, e.g., leading to the formation of a star (see Figure 1 for a visualization). However, accretion can happen only with an efficient mechanism for rapidly transporting angular momemtum outwards Julien & Knobloch (2010). It was suggested that turbulence drives angular momentum outwards but there was no known mechanism that would generate turbulence.

These Keplerian disks satisfies the Rayleigh stability criterion (see Rayleigh 1916) against centrifugal instability. Thus, there has to be other mechanisms that generates turbulence. Many instabilities such as barotropic Dubrull *et al.* (2005) and finite amplitude shear instabilities Dubrulle *et al.* (2005), Lesur & Longaretti (2005) etc have been suggested but none of them are sufficient

[t] 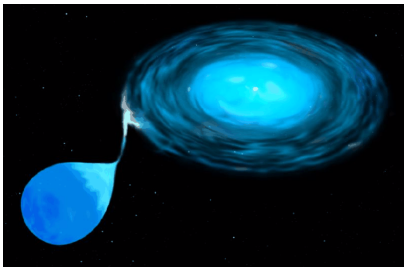

FIGURE 1. Artist's illustration of an accretion disk in a binary system. Taken from http://apod.nasa.gov/apod/ap991219.html.

for the angular momentum transport outward required Ji *et al.* (2006). Magnetic field-induced instabilities MRI seem to be the most promising.

MRI is a linear instability that is triggered by weak poloidal magnetic field. It is axisymmetric and occurs in Rayleigh-stable regime where the angular velocity decreases outwards, which is the case for the accretion we are interested in. The efficiency of angular momentum transport depends on the saturation of MRI Balbus & Hawley (1991), Balbus & Hawley (1998).

MRI is not only applicable to astrophysical phenomena but geophysical ones as well, e.g. the Earth's magnetic field Petitdemange *et al.* (2008). It is used to better understand how planetary magnetic field might have formed on Earth or other planets and how the field is sustained or decayed through time.

In this report, we attempt to explain and illustrate the instability in an astrophysical sense and go through what has been done experimentally and numerically in terms of MRI.

2. Background

2.1. *Perfectly conducting fluid in magnetic field*

The magnetic field lines are tied to the conducting fluid in which they are embedded. We can show this by comparing a transport equation of magnetic field with a equation for a line element moving with fluid. We first combine Ohm's Law in ideal conductor and Faraday's equation to get a transport equation for magnetic field,

$$\begin{aligned}\frac{\partial \mathbf{B}}{\partial t} &= \nabla \times (\mathbf{u} \times \mathbf{B}) \\ &= \mathbf{B} \cdot \nabla \mathbf{u} - \mathbf{u} \cdot \nabla \mathbf{B} - \mathbf{B} \nabla \cdot \mathbf{u}. \end{aligned} \tag{2.1}$$

Assuming incompressibility, we get

$$\frac{D\mathbf{B}}{Dt} = (\mathbf{B} \cdot \nabla)\mathbf{u}, \tag{2.2}$$

where $\frac{D}{Dt}$ is the convective derivative defined as

$$\frac{D}{Dt} = \frac{\partial}{\partial t} + (\mathbf{u} \cdot \nabla) \tag{2.3}$$

Considering a short line element $d\mathbf{l}$ moving with fluid, we can express the rate of change of $d\mathbf{l}$ as

$$\frac{D}{Dt}(d\mathbf{l}) = \mathbf{u}(\mathbf{x} + d\mathbf{l}) - \mathbf{u}(\mathbf{x}) = (d\mathbf{l} \cdot \nabla)\mathbf{u}. \tag{2.4}$$

Comparing two equations above, we can conclude that $\mathbf{B}$ and $d\mathbf{l}$ obey the same equation (see Davidson 2001). Therefore, the field lines are frozen into the fluid.

2.2. *Magnetic tension*

When the fluid elements are displaced from their equilibrium position, the magnetic field lines move together with fluid elements and behave like elastic bands frozen-into the fluid. Using Ampere's law, the Lorenz force ($\mathbf{J} \times \mathbf{B}$) may be written as

$$\mathbf{J} \times \mathbf{B} = -\nabla \left(\frac{B^2}{2\mu} \right) + \frac{(\mathbf{B} \cdot \nabla)\mathbf{B}}{\mu} = -\nabla \left(\frac{B^2}{2\mu} \right) + \frac{\partial}{\partial s} \left[\frac{B^2}{2\mu} \right] \hat{e}_t - \frac{B^2}{\mu R} \hat{e}_n \tag{2.5}$$

where R is radius of curvature, s is a coordinate along a magnetic field line, and $\hat{e}_t$ and $\hat{e}_n$ are tangential and normal unit vectors respectively. The last two terms are magnetic tension forces in tangential and normal directions. These forces can also be interpreted as tensile stress of $B^2/2\mu$ acting on the end of the tube (see Davidson 2001).

This tensile force which is also know as Faraday or Maxwell tension is analogous to a force acting on a spring. Considering a displacement $\boldsymbol{\xi} = \mathbf{v}\delta t$, the Faraday's equation can be written as $\delta\mathbf{B} = ikB\boldsymbol{\xi}$. The magnetic tension for small displacement per unit density ρ is

$$\frac{(\mathbf{B} \cdot \nabla)\delta\mathbf{B}}{\mu\rho} = \frac{ikB\delta\mathbf{B}}{\mu\rho} = -\frac{k^2 B^2}{\mu\rho}\boldsymbol{\xi} = -K\boldsymbol{\xi}, \tag{2.6}$$

where K is comparable to the spring constant (see Wikipedia 2013; Balbus & Hawley 1998). The equation has same form of Hooke's Law for a spring.

2.3. *Magnetoroational instability*

We present a relatively simple physical explanation of the magnetorotational instability from Balbus (2011). Consider Keplerian motion of conducting fluid orbiting around a central body of mass M_c.Two adjacent fluid elements m_i and m_o, at radial position r_i and r_o, are orbiting around gravitational center with angular velocities $\Omega_i = \sqrt{GM_c/r_i^3}$ and $\Omega_o = \sqrt{GM_c/r_o^3}$ respectively. Therefore the angular velocity of the inner element is higher than that of the outer elements $\left(d\Omega^2/dr < 0\right)$, but the angular momentum of the inner element is smaller than that of the outer element $\left(dr^4\Omega^2/dr > 0\right)$.

If a magnetic field line is connecting the conducting fluid elements, the magnetic field will move together with the two elements. Because of the velocity shear in Keplerian motion, the magnetic field will be stretched and bent. Therefore the magnetic field will exert restoring force on the fluid element making the inner element pulled back and the outer element dragged forward. The inner element lose angular momentum, therefore it must fall to an orbit of smaller radius. On the other hand the outer element gains angular momentum and moves to the orbit of larger radius (see Balbus 2011; Wikipedia 2013). This outward angular momentum transport makes the small initial displacement get larger. The magnetic fields are stretched even more and gives positive feedback leading the system unstable. This instability is known as a magnetorotational instability (MRI) and is illustrated in Figure 2.

One can show that the dispersion relation for the incompressible ideal flow rotating with angular velocity Ω_0 is

$$\omega^4 - \left[2\left(k^2 V_A^2\right) + \kappa^2\right]\omega^2 + \left(k^2 V_A^2\right)\left[\left(k^2 V_A^2\right) + r\frac{d\Omega^2}{dr}\right] = 0, \tag{2.7}$$

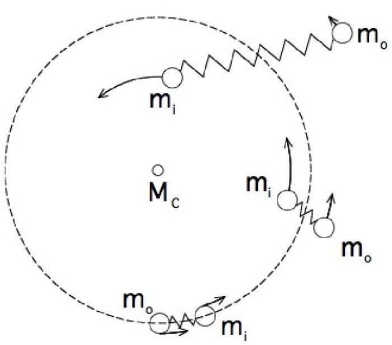

[t]

FIGURE 2. A schematic diagram from Balbus (2011) showing magnetorotational instability. Two fluid elements m_i (inner) and m_o (outer) orbit a mass (M_C) with the magnetic tension between the two elements represented by a spring. Over time m_i loses angular momentum, moving closer to M_C while m_o gains angular momentum and moves away from M_C.

where ω and k are angular frequency and wave number of a perturbation $\xi \propto e^{i(kz+\omega t)}$, $V_A = B/\sqrt{\mu\rho}$ is Alfvén speed for the imposed magnetic field B, and κ^2 is the epicylic frequency, defined as

$$\kappa^2 = 4\Omega_0^2 + r\frac{d\Omega^2}{dr} \tag{2.8}$$

See Balbus & Hawley (1991, 1998); Balbus (2003) for more details. If $d\Omega^2/dr < 0$, then one of ω^2 has negative root for long wave length modes satisfying

$$k^2 < -\frac{r}{V_A^2}\frac{d\Omega^2}{dr}. \tag{2.9}$$

Therefore, the instability criterion for the magnetorotational instability (MRI) is represented as radially decreasing angular velocity,

$$\frac{d\Omega^2}{dr} < 0 \quad \text{(UNSTABLE)} \tag{2.10}$$

Note that the MRI is different from the conventional hydrodynamic instability known as Couette-Taylor centrifugal instability. The Couette-Taylor centrifugal instability criterion for axsymmetric perturbation is represented as radially decreasing angular momentum (see Charru & de Forcrand-Millard 2011):

$$\frac{dr^4\Omega^2}{dr} < 0 \quad \text{(UNSTABLE)} \tag{2.11}$$

The Keplerian disk is a good example of flows which are stable to the hydrodynamic instability but unstable to the MRI.

3. Theoretical Work

Acheson & Hide (1973) and Knobloch (1992) showed the linear stability analysis of rotating magneto-fluid bounded in coaxial cylinder. For the case of gaseous astrophysical disks in unbounded geometry was shown in Balbus & Hawley (1991). The condition for stability was shown to be radially

increasing angular velocity profile. We present a linear stability analysis of MRI for radially bounded case following Acheson (1972), Acheson (1973), Knobloch (1992), and Julien & Knobloch (2010).

3.1. *Governing equation*

The wave dispersion equation of a cylindrical magneto-fluid can be obtained from the magnetohydrodynamic (MHD) equations. Assuming the fluid is inviscid and perfectly conducting, the ideal MHD equations are

$$\rho\left(\frac{\partial \mathbf{u}}{\partial t}+\mathbf{u}\cdot\nabla\mathbf{u}\right)=-\nabla p+\mathbf{J}\times\mathbf{B} \tag{3.1}$$

$$\frac{\partial \rho}{\partial t}+\nabla\cdot(\rho\mathbf{u})=0 \tag{3.2}$$

$$\frac{d}{dt}\left(\frac{p}{\rho^{\gamma}}\right)=0 \tag{3.3}$$

$$\mathbf{E}+\mathbf{u}\times\mathbf{B}=0 \tag{3.4}$$

$$\nabla\times\mathbf{E}=-\frac{\partial \mathbf{B}}{\partial t} \tag{3.5}$$

$$\nabla\times\mathbf{B}=\mu\mathbf{J}, \tag{3.6}$$

where $\mathbf{u}$ fluid velocity, ρ is fluid denstity, p is pressure. $d/dt=\partial/\partial t+\mathbf{u}\cdot\nabla$ is convective derivative and γ is the ratio of specific heats. $\mathbf{E}$, $\mathbf{B}$ and $\mathbf{J}$ are electic field, magnetic field and current density respectively (see Freidberg 1987).

To investigate the magnetorotational instability, one can consider homogeneous incompressible fluid rotating with angular velocity $\Omega(r)=V(r)/r$ in externally imposed magnetic fields $\mathbf{B}_0=[0,B_\phi(r),B_z(r)]$. Combining electromagnetic equations with momentum relation, we get the appropriate MHD equations,

$$\frac{\partial \mathbf{u}}{\partial t}+(\mathbf{u}\cdot\nabla)\mathbf{u}=-\frac{1}{\rho}\nabla\left(P+\frac{\mathbf{B}^2}{2\mu}\right)+\frac{1}{\mu\rho}(\mathbf{B}\cdot\nabla)\mathbf{B} \tag{3.7}$$

$$\frac{\partial \mathbf{B}}{\partial t}+(\mathbf{u}\cdot\nabla)\mathbf{B}=(\mathbf{B}\cdot\nabla)\mathbf{u} \tag{3.8}$$

$$\nabla\cdot\mathbf{u}=0 \tag{3.9}$$

$$\nabla\cdot\mathbf{B}=0. \tag{3.10}$$

3.2. *Linear perturbation equation and eigenvalue problem*

We can get linearized equations by perturbing the basic state by small amount of $\mathbf{u_1}$ and $\mathbf{b_1}$ for velocity and magnetic fields. The linear perturbation is assumed to have the form

$$f=\Re\left[\hat{f}(r)e^{i(m\phi+kz+\omega t)}\right]. \tag{3.11}$$

According to Acheson (1972), the normal mode equations are

$$\hat{b}_r = \frac{\hat{u}_r}{\omega}\left(kB_z + \frac{mB_\phi}{r}\right) \tag{3.12}$$

$$\hat{b}_\phi = -\frac{(\hat{u}_r B_\phi)'}{i\omega} + \frac{k}{\omega}(\hat{u}_\phi B_z - \hat{u_z} B_\phi) \tag{3.13}$$

$$\hat{b}_z = -\frac{(r\hat{u}_r B_z)'}{ri\omega} - \frac{m(\hat{u_\phi} B_z - \hat{u}_z B_\phi)}{r\omega} \tag{3.14}$$

$$\hat{u}_z = -\frac{(r\hat{u}_r)'}{rik} - \frac{m\hat{u}_\phi}{rk} \tag{3.15}$$

$$\left(1 + \frac{m^2}{r^2k^2}\right) ri\hat{u}_\phi = -\frac{m}{rk^2}(r\hat{u}_r)' - \frac{\hat{u}_r}{\left(V_{Az} + \frac{mV_{A\phi}}{rk}\right)^2 \frac{k^2}{\omega^2} - 1}\left\{-\frac{2\Omega r}{\omega} + \frac{2kV_{A\phi}}{\omega^2}\left(V_{Az} + \frac{mV_{A\phi}}{rk}\right)\right\} \tag{3.16}$$

where $V_{A\phi} = B_\phi(r)/\sqrt{\mu\rho}$ and $V_{Az} = B_z(r)/\sqrt{\mu\rho}$ are Alfvén speeds for associated external magnetic field components.

Solving the normal mode equation set for radial velocity perturbation $\hat{u}_r = u$ and considering axisymmetric perturbation ($m = 0$), Acheson (1973) obtained following eigenvalue problem,

$$\frac{d}{dr}\left[(\omega^2 - k^2V_{Az}^2)\left(\frac{du}{dr} + \frac{u}{r}\right)\right] - k^2\left[\omega^2 - k^2V_{Az}^2 + r\frac{d}{dr}\left(\frac{V_{A\phi}^2}{r^2} - \frac{V^2}{r^2}\right)\right]u = -\frac{4k^2}{r^2}\frac{(kV_{A\phi}V_{Az} + \omega V)^2}{(\omega^2 - k^2V_{Az}^2)}u. \tag{3.17}$$

3.3. *Stability criterion*

3.3.1. *Standard magnetorotational instability*

Consider a standard MRI of radially bounded coaxial fluid cylinder with externally imposed axial magnetic field but without axial current flowing. Therefore, we have $V_{Az} = \text{constant} \neq 0$ and $V_{A\phi} = 0$. Considering boundary condition $u(r_1) = u(r_2) = 0$, we multiply the eigenvalue equation by complex conjugate of u and integrate over radial coordinate,

$$(\omega^2 - k^2V_{Az}^2)^2 = \frac{k^2}{D}\int_{r_1}^{r_2}\left[\frac{\omega^2}{r^2}\frac{d}{dr}r^2V^2 - r^2k^2V_{Az}^2\frac{d}{dr}\left(\frac{V^2}{r^2}\right)\right]|u|^2dr \tag{3.18}$$

where

$$D \equiv \int_{r_1}^{r_2}\left(r\left|\frac{du}{dr}\right|^2 + \frac{|u|^2}{r} + k^2r|u|^2\right)dr > 0 \tag{3.19}$$

According to Chandrasekhar (1960), ω^2 must be real. We get stable modes with $\omega^2 > 0$ and unstable modes with $\omega^2 < 0$. If the angular velocity increases radially outward, $\frac{d}{dr}\left(\frac{V^2}{r^2}\right) > 0$, the system is stable because ω^2 is bounded from below by positive number,

$$\omega^2 > \frac{r^2k^2V_{Az}^2\frac{d}{dr}\left(\frac{V^2}{r^2}\right)}{4\frac{V^2}{r} + r^2\frac{d}{dr}\left(\frac{V^2}{r^2}\right)} > 0. \tag{3.20}$$

If we have radially decreasing angular velocity profile, $\frac{d}{dr}\left(\frac{V^2}{r^2}\right) < 0$, somewhere $r_1 < r < r_2$, then ω^2 may have negative solution which makes the system unstable.

3.3.2. *Helical magnetorotational instability*

When the external nonzero magnetic fields in axial and azimuthal directions are considered, it was found that the eigenvalue equation can be written as

$$\frac{d}{dr}r\frac{du}{dr} - \frac{u}{r} - k^2 ru = \frac{k^2}{(\omega^2 - k^2 V_{Az}^2)^2}\left[r^2\frac{d}{dr}\left(\frac{V_{A\phi}^2 - V^2}{r^2}\right)(\omega^2 - k^2 V_{Az}^2) - \frac{4}{r}(kV_{A\phi}V_{Az} - \omega V)^2\right]u \tag{3.21}$$

According to Knobloch (1992) and Julien & Knobloch (2010), the exponentially growing mode $\omega = -i\lambda$, $\lambda > 0$ is possible when the eigenvalue relation has the form

$$(\lambda^2 + k^2 V_{Az}^2)^2 = \frac{k^2}{D}\int_{r_1}^{r_2}\left[r^2\frac{d}{dr}\left(\frac{V_{A\phi}^2 - V^2}{r^2}\right)(\lambda^2 + k^2 V_{Az}^2) + \frac{4}{r}(kV_{A\phi}V_{Az} - i\lambda V)^2\right]|u|^2 dr. \tag{3.22}$$

Considering the imaginary part of the equation, we have

$$\int_{r_1}^{r_2}\frac{1}{r}V_\phi V|u|^2 dr = 0 \tag{3.23}$$

Knobloch (1992) showed that exponentially growing instability is only possible when $V_{A\phi}$ or V changes sign somewhere in $r_1 < r < r_2$.

4. Laboratory Experiments

Attempts to generate MRI in laboratory environments did not begin until 2001, four decades after the first magnetohydrodynamic (MHD) experiments (see Donnelley & Ozima 1960). In contrast to MRI, the first MHD experiments focused on stabilizing, rather than generating, instabilities within Taylor-Couette flow using magnetic fields. Experiments aimed at generating MRI were not devised until the after published work indicating MRI's role as the transport mechanism of angular momentum within accretion disks (need to add citation of paper).

4.1. *Standard magnetorotational instability*

Beginning with Ji *et al.* (2001), researchers have attempted to produce MRI by applying an axial magnetic field to a stable, quasi-Keplerian flow. Unfortunately, to-date no group has been able to experimentally genereate the standard MRI due to technical issues. Specifically, researchers have been unable to create an experimental setup which can withstand the required flow conditions for MRI (Ji *et al.* 2001; Goodman & Ji 2002). Additionally, researchers have had difficulty eliminating Ekman circulation within their setups, which can transport angular momentum and therefore whose presence can contaminate any experimental results Kageyama *et al.* (2004).

Although definitive identification of MRI has yet to be reported, Sisan *et al.* (2004) reported instabilities using a spherical Couette flow. The experimental setup applied a magnetic field coaxially to an inner rotating sphere with an outer fixed sphere and liquid sodium as the conducting fluid (see Figure 3). Once the magnetic field was increased beyond a threshold value, instabilities within the flow were observed which Sisan *et al.* (2004) classified as MRI. Gissinger *et al.* (2011) later numerically reproduced the results of Sisan *et al.* (2004), but identified the instabilities as shear

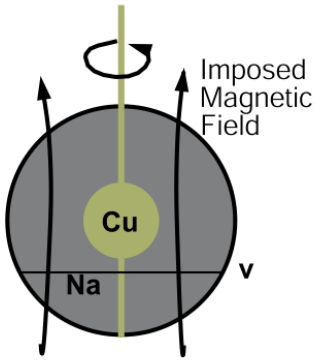

FIGURE 3. Diagram from Sisan *et al.* (2004) showing the experimental setup used to generate MRI. The fixed outer steel sphere contains liquid sodium (the conducting fluid), with the magnetic field imposed coaxially to the rotating inner copper sphere. The magnetic fields and fluid velocity are measured using Hall probes and Doppler velocimetry.

layer instabilities, aka the Schercliff layer, caused by the imposed magnetic field and the spherical boundaries. Unfortuntately, the spherical boundaries means the Schercliff layer are unlikely to be relevant to accretion disks which are not spherical.

4.2. *Helical magnetorotational instability*

As noted in Section 4.1, a difficulty with generation of MRI is attaining sufficient speeds without damaging the experimental setup. Although researchers are actively working on solving this issue, there are also several groups researching helical MRI (HMRI), a modified type of MRI which requires less extreme flow conditions. Although accretion disks do not exhibit azimuthal magnetic fields, HMRI experiments are still valuable in understand the underlying physics involved in MHD.

HMRI is MRI generated by applying both axial and azimuthal magnetic fields to a magnetized fluid, and was first proposed by Hollerbach & Rudiger (2005). Hollerbach's paper showed that the addition of an azimuthal magnetic field would allow MRI to be generated at Reynolds numbers 10^3 less than those of standard MRI. Generation of HMRI has since been experimentally proven by the PROMISE experiments (see Stefani *et al.* 2006, 2007, 2009, 2012). Figure 4 illustrates a typical experimental setup for generating HMRI.

5. Numerical Work

On top of experiments mentioned in the previous section, numerical simulations are also employed to try to explain the anomalous viscosity and magnetic field generation. Direct numerical simulations (DNS) are typically used with the advance of supercomputers and dramatically decreased computing time. DNS of the magnetohydrodynamics (MHD) Navier Stokes equations have had much success in the determination of the existence of MRI. Many of the numerical simulations assume axisymmetric, vertically global and incompressible flow if Alfven speed slower than sound speed as occurs in that regime that is stable to Taylor-Couette, the MHD equations can be simplified to be incompressible since it is not fundamental to the instability Balbus & Hawley (1991) with some exceptions Sano *et al.* (1998).

We begin with the widely used local shearing box model Balbus & Hawley (1991) which has

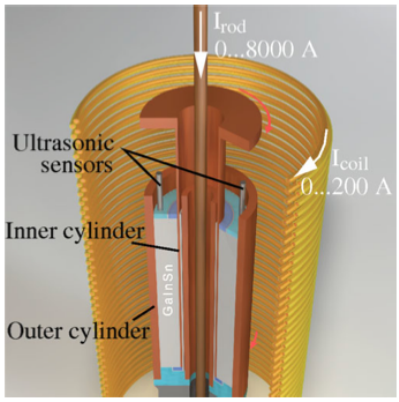

FIGURE 4. Diagram of a typical HMRI experimental setup from Ji (2010). The liquid metal is placed between the inner and outer cylinders, with imposed axial and azimuthal magnetic fields.

special properties of the model equations that makes it easier to simulate (see Figure 5). The special properties are that the toroidal field drops out, there is no distinction between inward and outward directions (symmetry) and MRI becomes an exponentially growing instability, which is what is needed Julien & Knobloch (2010).

Periodic boundary conditions were used with an added shearing component to the radial direction. "Method of characteristics-constrained transport" algorithm as explained in Hawley *et al.* (1995) was implemented. This model with an initial input magnetic field with zero- volume average initiates MRI but may obliterate the magnetic field and thus suppress the turbulence.

The comparison of the 3D simulations results from Hawley *et al.* (1995) with the 2D results from Balbus *et al.* (1994) shows significant difference. The 2D results have a general channel/streaming flow solution whereas the 3D results may go through the channel flow but eventually evolves further into a turbulent flow with some not going through the channel flow at all. Vertical component of gravity, hence buoyancy, was ignored and since their simulations showed significant density contrast, the shearing box model is not self-consistent. Purely hydrodynamic turbulence did not give significant angular momentum transport needed even when the initial conditions had strong turbulence structures. Their 3D results suggest that accretion disks are well described by Euler's, ignoring the viscous terms from Navier Stokes Hawley *et al.* (1995).

There are many variations of numerical simulations using the local shearing box model with results worth learning from. Fromang & Papaloizou (2007) and Fromang *et al.* (2007) have shown that numerical results using the box model with zero net flux are highly dependent on the numerical method used and resolution of the grid unless explicit diffusion coefficients and the appropriate dissipative scales are resolved . This issue has been considered in Lesur & Longaretti (2007) for cases with nonzero net vertical flux, where they found that both the viscosity and resistivity affect the amount of angular momentum transported by magnetohydrodynamic turbulence.

Sano *et al.* (1998) has shown that whether saturation occurs depends on the Elsasser number $\Delta \equiv v_A^2/\eta\Omega$, which describes the relative balance of Lorentz forces to Coriolis forces. Non-axisymmetric numerical simulations done by Fleming *et al.* (2000) suggest saturation does occur even when Elsasser number $\Delta \geq 1$ if non-axisymmetric disturbances are allowed to evolve.

Other variations of the shearing box models include vertically stratified disks as done in Miller & Stone (1999), who found that turbulent magnetised disk can produce a magnetised corona in

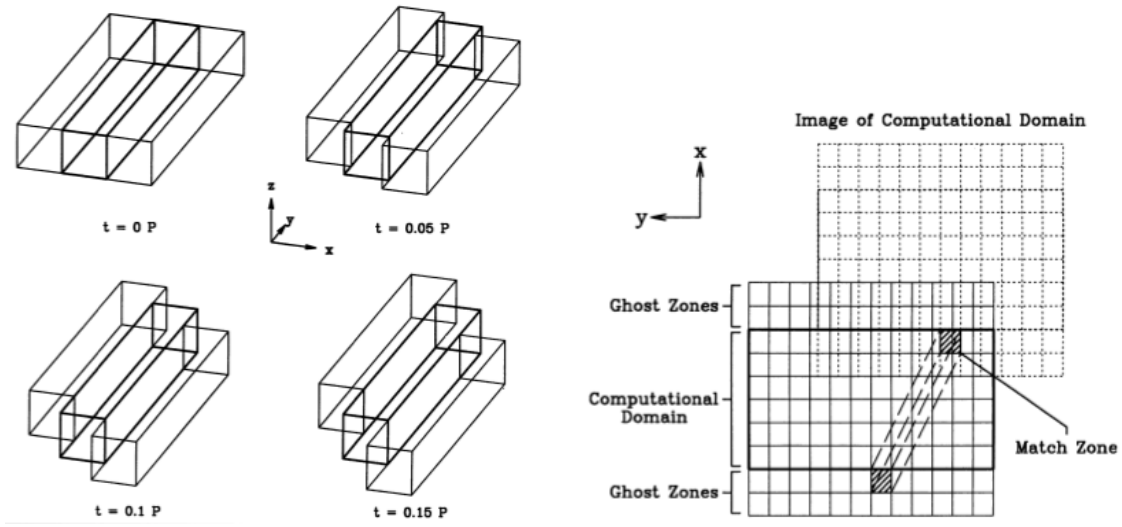

FIGURE 5. Diagram (left) and boundary conditions (right) of the shearing box model from Balbus & Hawley (1991).

.

laminar flow through MRI. Stone *et al.* (1996) presented a 3D MHD simulation of the nonlinear evolution of MRI in a local shearing box method with a global vertical direction and vertically stratified disk as well. They found that the instability generated and maintained MHD turbulence.

The use of the shearing box model has its limitations as pointed out by Hawley *et al.* (1995) Regev & Umurhan (2008) as they do not permit any dynamics involving the background shear, which is taken as imposed and constant in space and time (Regev & Umurhan 2008). With regards to resolution which is tied in with the model used, the efficiency of angular momentum transport appears to decrease with improved resolution as shown by Fromang *et al.* (2007), suggesting that transport rates estimated on basis of ideal MHD are affected by grid-scale dissipation and overestimate the efficiency of angular momentum extraction by MRI. Kapyla & Korpi (2011) also worked on resolution dependence of α, the Shakura-Sunyaev number and the possible decline of the angular momentum transport rate with decreasing Pm. Even though the shearing box model is restrictive in resolving the behavior of the accretion disk, it is nonetheless useful in obtaining actual evidence for MRI Balbus & Hawley (1998) (see Figure 6) and understanding the dynamo process that sustains the magnetic field in planetary systems Lesur & Ogilvie (2008).

Kirillov *et al.* (2012) presents a unifying description of the helical and azimuthal versions of MRI, and they also identify the universal character of the 'Liu' limit $2(1-2) \approx -0.8284$ for the critical Rossby number. From this universal characteristics, they are led to the prediction that the instability will be governed by a mode with an azimuthal wavenumber that is proportional to the ratio of axial to azimuthal applied magnetic field, when this ratio becomes large and the Rossby number is close to the Liu limit)

Apart from the local shearing box model, other 3D models have been implemented as well. Liu (2008) simulated nonlinear development of MRI in a non-ideal magnetohydrodynamic Taylor-Couette flow (mimicking an on-going Princeton MRI experiment) using ZEUS-MP 2.0 code (Hayes *et al.* (2006)), which is a time-explicit, compressible, astrophysical ideal MHD parallel 3D code with

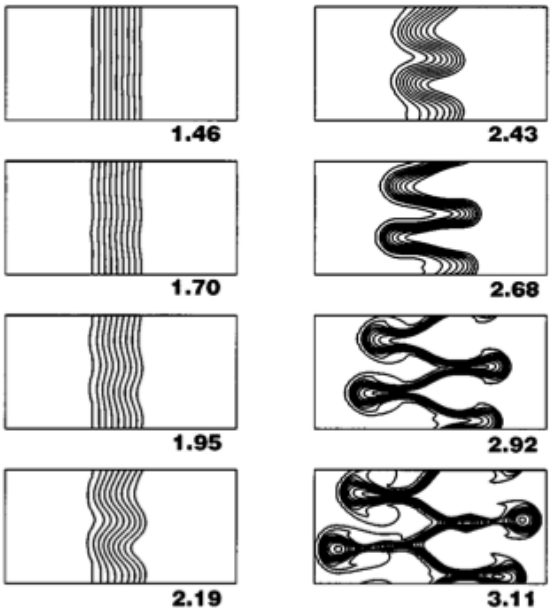

FIGURE 6. Numerical results from Balbus & Hawley (1998) showing the temporal evolution of MRI. The snapshots are (R, z) cross-sections of field lines, with the origin at the bottom left, and the time in number of orbits annotated to each snapshot.

added viscosity and resistivity for axisymmetric flows in cylindrical coordinates. He shows that the saturation of MRI causes a inflowing 'jet' feature which is opposite to the usual Ekman circulation and enhances angular momentum transport radially outward, which is what is needed, agreeing with Hawley *et al.* (1995). Stable MRI regime ($Re \leq 1600$) enhances vertical angular momentum transport while in unstable MRI regime ($Re \geq 3200$), MRI kicks in, resulting in more radial angular momentum transport as compared with vertical Liu (2008).

Other general relativistic global 3D MHD codes have been implemented to show the existence of MRI and explore other astronomical phenomena De Villiers & Hawley (2003),Koide *et al.* (2000). Kersale *et al.* (2006) simulated global MRI to look more into the nonlinear properties and the formation of a jet that transports vertical magnetic flux. A 3D hydrodynamic simulations explores the nonlinear evolution of vertical shear instability in accretion disk and finds that vertical dependence destabilizes the disk, leading to velocity fluctuations that increases angular momentum transport Arlt & Urpin (2004), contrary to Hawley *et al.* (1995).

6. Conclusion

Concluding remarks

REFERENCES

ACHESON, D.J. 1972 On the hydromagnetic stability of a rotating fluid annulus. *Journal of Fluid Mechanics* **52**, 529–541.

Acheson, D.J. 1973 Hydromagnetic wavelike instabilities in a rapidly rotating stratified fluid. *Journal of Fluid Mechanics* **61**, 609–624.

Acheson, D.J. & Hide, R. 1973 Hydromagnetics of rotating fluids. *Reports on Progress in Physics* **36** (2), 159.

Arlt, R. & Urpin, V. 2004 Simulations of vertical shear instability in accretion discs. *Astron. Astrophys* **426**, 755765.

Balbus, S.A., Gammie, C.F. & Hawley, J.F. 1994 Fluctuations, dissipation and turbulence in accretion discs. *Monthly Notices of the Royal Astronomical Society* **271**, 197–201.

Balbus, S.A. & Hawley, J.F. 1991 A powerful local shear instability in weakly magnetized disks. i - linear analysis. ii - nonlinear evolution. *Astrophysical Journal* **376**, 214–233.

Balbus, S. A. 2003 Enhanced angular momentum transport in accretion disks. *Ann. Rev. Astron. Astrophys* **41**, 555–597.

Balbus, S. A. 2011 *Magnetohydrodynamics of Protostellar Disks*, pp. 237–282.

Balbus, Steven A. & Hawley, John F. 1998 Instability, turbulence, and enhanced transport in accretion disks. *Rev. Mod. Phys.* **70**, 1–53.

Chandrasekhar, S. 1960 The stability of non-dissipative couette flow in hydromagnetics. *Proceedings of the National Academy of Science* **46**, 253–257.

Charru, Francois & de Forcrand-Millard, Patricia 2011 *Hydrodynamic instabilities*, , vol. 37. Cambridge University Press.

Davidson, Peter Alan 2001 *An introduction to magnetohydrodynamics*, , vol. 25. Cambridge university press.

De Villiers, J.P. & Hawley, J.F. 2003 A numerical method for general relativistic magnetohydrodynamics. *The Astrophysical Journal* **589**, 458–480.

Donnelley, R.J. & Ozima, M. 1960 Hydromagnetic stability of flow between rotating cylinders. *Phys. Rev. Lett.* **4**, 497–498.

Dubrull, B., Marie, L., Normand, Ch., Richard, D., Hersant, F. & Zahn, J.-P. 2005 A hydrodynamic shear instability in stratified disks. *Astron. Astrophys.* **429**, 1–13.

Dubrulle, B., Dauchot, O., Daviaud, F., Longaretti, P.-Y., Richard, D. & Zahn, J.-P. 2005 Stability and turbulent transport in taylor-couette flow from analysis of experimental data. *Phys. Fluids* **17**, 1070–6631.

Fleming, T.P., Stone, J.I.M. & Hawley, J.F. 2000 The effect of resistivity on the nonlinear stage of the magnetorotational instability in accretion disks. *Astrophysical Journal* **530**, 464–477.

Freidberg, Jeffrey P. 1987 *Ideal magnetohydrodynamics*. Plenum Press, New York, NY.

Fromang, S. & Papaloizou, J. 2007 Mhd simulations of the magnetorotational instability in a shearing box with zero net flux. *Astronomy & Astrophysics* **476** (3), 1113–1122.

Fromang, S., Papaloizou, J., Lesur, G. & Heinemann, T. 2007 Mhd simulations of the magnetorotational instability in a shearing box with zero net flux - the effect of transport coefficients. *Astronomy & Astrophysics* **476** (3), 1123–1132.

Gissinger, Christophe, Ji, Hantao & Goodman, Jeremy 2011 Instabilities in magnetized spherical couette flow. *Phys. Rev. E* **84**, 026308.

Goodman, J. & Ji, H.T. 2002 Magnetorotational instability of dissipative couette flow. *Journal of Fluid Mechanics* **462**, 365–382.

Hawley, J.F., Gammie, C.F. & Balbus, S.A. 1995 Local 3-dimensional magnetohydrodynamic simulations of accretion disks. *Astrophysical Journal* **440**, 742–763.

Hayes, John C., Norman, Michael L., Fiedler, Robert A., Bordner, James O., Li, Pak Shing, Clark, Stephen E., ud Doula, Asif & Mac Low, Mordecai-Mark 2006 Simulating radiating and magnetized flows in multiple dimensions with zeus-mp. *Astrophysical Journal Supplement Series* **165** (1), 188–228.

Hollerbach, Rainer & Rudiger, Gunther 2005 New type of magnetorotational instability in cylindrical taylor-couette flow. *Physical Review Letters* **95**.

Ji, Hantao 2010 Current status and future prospects for laboratory study of angular momentum transport relevant to astrophysical disks. *Proceedings of the International Astronomical Union* **6**, 18–25.

Ji, H., Burin, M., Schartman, E. & Goodman, J. 2006 Hydrodynamic turbulence cannot transport angular momentum effectively in astrophysical disks. *Nature* **444**, 343–346.

Ji, H.T., Goodman, J. & Kageyama, A. 2001 Magnetorotational instability in a rotating liquid metal annulus. *Monthly Notices of the Royal Astronomical Society* **325** (2), L1–L5.

Julien, K. & Knobloch, E. 2010 Magnetorotational instability: recent developments. *Philosophical Transactions of the Royal Society A* **368**, 1607–1633.

Kageyama, Akira, Ji, Hantao, Goodman, Jeremy, Chen, Fei & Shoshan, Ethan 2004 Numerical and experimental investigation of circulation in short cylinders. *Journal of the Physical Society of Japan* **73** (9), 2424–2437.

Kapyla, P.J. & Korpi, M.J. 2011 Magnetorotational instability driven dynamos at low magnetic prandtl numbers. *Monthly Notices of the Royal Astronomical Society* **413** (2), 901–907.

Kersale, E., Hughes, D. W., Ogilvie, G. I. & Tobias, S. M. 2006 Global magnetorotational instability with inflow. ii. the non-linear development of axisymmetric wall modes. *Astrophys. J.* **638**, 382–390.

Kirillov, Oleg N., Stefani, Frank & Fukumoto, Yasuhide 2012 A unifying picture of helical and azimuthal magnetorotational instability, and the universal significance of the liu limit. *The Astrophysical Journal* **756** (1), 83.

Knobloch, E. 1992 On the stability of magnetized accretion discs. *Monthly Notices of the Royal Astronomical Society* **255**, 25P–28P.

Koide, S., Meier, D. L., Shibata, K. & Kudoh, T. 2000 General relativistic simulations of early jet formation in a rapidly rotating black hole magnetosphere. *Astrophysical Journal* **536**, 668–674.

Lesur, G. & Longaretti, P.Y. 2007 Impact of dimensionless numbers on the efficiency of magnetorotational instability induced turbulent transport. *Monthly Notices of the Royal Astronomical Society* **378** (4), 1471–1480.

Lesur, G. & Longaretti, P. Y. 2005 On the relevance of subcritical hydrodynamic turbulence to accretion disk transport. *Astron. Astrophys.* **444**, 25–44.

Lesur, Geoffroy & Ogilvie, Gordon I. 2008 Localized magnetorotational instability and its role in the accretion disc dynamo. *Monthly Notices of the Royal Astronomical Society* **391** (3), 1437–1450.

Liu, Wei 2008 Numerical study of the magnetorotational instability in princeton mri experiment. *The Astrophysical Journal* **684** (1), 515.

Miller, K.A. & Stone, J.M. 1999 3d mhd simulations of the magneto-rotational instability in vertically stratified disks. *Numerical Astrophysics* .

Petitdemange, L., Dormy, E. & Balbus, S. A. 2008 Magnetostrophic mri in the earth's outer core. *Geophys. Res. Lett.* .

Rayleigh, Lord 1916 On convection currents in horizontal layer of fluid when the higher temperature is on the under side. *Phil. Mag.* **32**, 529–546.

Regev, O. & Umurhan, O.M. 2008 On the viability of the shearing box approximation for numerical studies of mhd turbulence in accretion disks. *Astronomy & Astrophysics* **481** (1), 21–32.

Sano, T., Inutsuka, S. & Miyama, S. M. 1998 A saturation mechanism of magnetorotational instability due to ohmic dissipation. *The Astrophysical Journal* **506**, L57–L60.

Sisan, Daniel R., Mujica, Nicolás, Tillotson, W. Andrew, Huang, Yi-Min, Dorland, William, Hassam, Adil B., Antonsen, Thomas M. & Lathrop, Daniel P. 2004 Experimental observation and characterization of the magnetorotational instability. *Phys. Rev. Lett.* **93**, 114502.

Stefani, F., Eckert, S., Gerbeth, G., Giesecke, A., Gundrum, Th., Steglich, C., Weier, T. & Wustmann, B. 2012 DRESDYN - a new facility for mhd experiments with liquid sodium. *Magnetohydrodynamics* **48** (1), 103–113, 8th PAMIR International Conference on Fundamental MHD and Liquid Metal Technology, Borgo Corsica, France, SEP 05-09, 2011.

Stefani, Frank, Gerbeth, Gunter, Gundrum, Thomas, Hollerbach, Rainer, Priede, Janis, Rüdiger, Günther & Szklarski, Jacek 2009 Helical magnetorotational instability in a taylor-couette flow with strongly reduced ekman pumping. *Phys. Rev. E* **80**.

Stefani, Frank, Gundrum, Thomas, Gerbeth, Gunter, Rüdiger, Günther, Schultz, Manfred, Szklarski, Jacek & Hollerbach, Rainer 2006 Experimental evidence for magnetorotational instability in a taylor-couette flow under the influence of a helical magnetic field. *Phys. Rev. Lett.* **97**.

Stefani, Frank, Gundrum, Thomas, Gerbeth, Gunter, Rdiger, Gnther, Szklarski, Jacek &

Hollerbach, Rainer 2007 Experiments on the magnetorotational instability in helical magnetic fields. *New Journal of Physics* **9** (8).

Stone, J.M., Hawley, J.F., Gammie, C.F. & Balbus, S.A. 1996 Three-dimensional magnetohydrodynamical simulations of vertically stratified accretion disks. *The Astrophysical Journal* **463** (2), 656–673.

Velikhov, E.P. 1959 Stability of an ideally conducting liquid flowing between cylinders rotating in a magnetic field. *Soviet Physics JETP-USSR* **9** (5), 995–998.

Wikipedia 2013 Magnetorotational instability — Wikipedia, the free encyclopedia. [Online; accessed 29-May-2013].